Natural convection in droplet evaporation

J. J. Hegseth
Department of Physics, University of New Orleans, New Orleans, Louisiana 70148

N. Rashidnia and A. Chai
Space Experiment Division, NASA Lewis Research Center, MS 500-102 Cleveland, Ohio 44135

(Received 3 April 1995)

Although droplet evaporation is widely assumed to be a diffusion process, our results show that when a droplet evaporates sufficiently fast it exhibits a vigorous interior flow. This flow is driven by surface tension gradients. The typical interior flow field behavior is shown as well as measurements of the droplet surface area and volume as it evaporates. We also discuss the droplet lifetime and how the system tends toward a state of marginal stability. [S1063-651X(96)03908-6]

PACS number(s): 47.20.Dr, 47.27.Te, 47.55.Dz

INTRODUCTION

Droplet evaporation occurs in many important natural and engineering processes. These include such diverse phenomena as cloud physics [1], combustion of fuel [2], biological crystal growth [3], heat radiators [4], etc. The first theory of the evaporation of a droplet in a gaseous media was presented by Maxwell [5]. He considered the simple case of a spherical droplet with its center of mass motionless with respect to a gaseous exterior. This diffusion theory of spherical droplet evaporation leads to his d^2 law: the square of the diameter d (or, equivalently, the radius r) of the droplet decreases linearly with time [5,6]. This theory assumes that the evaporation process is controlled by a mass diffusion process exterior to the droplet and leads to a total droplet lifetime t_l of $t_l = R^2\rho/2D\Delta c$ (R is the initial radius of the spherical droplet, ρ is the density of the evaporating media, D is the mass diffusion constant of the droplet material in the exterior gas, and Δc is the concentration change of the droplet material from the droplet surface to the ambient concentration far away from the droplet). Although Maxwell's law is derived from considering the exterior gas, a similar relation can be obtained by considering the interior liquid of the droplet. Although many more refined theoretical developments have included the effects of droplet center of mass motion, nonspherical droplets, etc. [6], they have all focused on the mass diffusion in the exterior gas of the droplet. While there have been previous observations of convection from evaporation in pools of liquid [7] and drops on flat plates [8], there have been no previous investigations of convection in the simple configuration of an evaporating droplet surrounded by gas. In the following we report such a flow in an evaporating droplet.

As an evaporating droplet decreases in mass, convection, and diffusion processes in the exterior gas medium transport the droplet mass away from the evaporating droplet [6]. The change of phase of the liquid to a gas at the surface requires an input heat called the latent heat of vaporization. In general, it is possible to have a heat flux into the surface from both the external gas and the internal liquid through conduction, convection, or radiation. Often radiative heat transfer is a smaller effect than conduction and convection. In most materials heat conducts much faster in the liquid phase than in the gas phase. If there is no convection, then the liquid interior of the evaporating droplet must supply the heat to the surface for vaporization. A temperature gradient normal to the evaporating droplet's surface develops as heat is rapidly conducted toward the surface. The conductive state has the potential to become unstable [9,10] because of the surface tension dependence on temperature (in most cases the surface tension decreases with increasing temperature).

A nonuniform temperature distribution at the surface creates a surface tension gradient that produces a forcing in which surface fluid is pulled toward regions of higher surface tension. The viscous force then transports momentum into the interior of the droplet and a convective flow results throughout the droplet. This surface tension driven instability is called the Marangoni instability [7,9,10]. A moving surface should also drive convection exterior to the droplet increasing the exterior mass and heat transport. This increased heat and mass transport should increase the evaporation rate. On the other hand, the convection should also tend to equilibrate the temperature at the surface decreasing any surface tension gradients and therefore tend to stop the convection.

A surface tension gradient results in a Marangoni flow only if there are no other forces to balance it. A stationary surface element that is perturbed into motion, however, has a viscous resistive force applied to it. A dimensionless number that measures the relative strengths (the ratio) of these opposing forces [(surface tension force)/(viscous resistive force)] is the Marangoni number Ma. The Marangoni number is $\mathrm{Ma} = \Delta\sigma R/\rho\upsilon\alpha$, where σ is the surface tension, $\Delta\sigma$ is the surface tension change along the interface (which must be present for there to exist any possibility for surface tension driven flow), ρ is the density, υ is the kinematic viscosity, α is the thermal diffusivity, and R is the radius of the droplet, which is the characteristic length over which the surface tension change $\Delta\sigma$ occurs. The Marangoni instability is characterized by a critical value of the Marangoni number Ma_c, which is the value where neither surface tension nor viscosity dominates. When $\mathrm{Ma} < \mathrm{Ma}_c$ the viscous force dominates and the surface perturbations dissipate. If $\mathrm{Ma} > \mathrm{Ma}_c$, however, the surface tension force dominates the viscous force and surface perturbations grow. The viscous force then

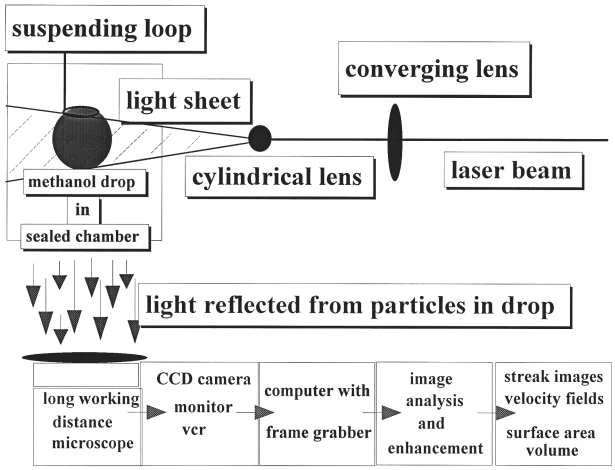

FIG. 1. The data shown in Figs. 2–4 are obtained using the laboratory setup shown schematically in this figure. Light from a He-Ne laser is focused using a converging lens such that the waist of the beam occurs at the droplet. The beam then goes through a cylindrical lens to form a light sheet. This light sheet is approximately 0.1 mm thick in the droplet (where the thickness is defined as the full width at half the maximum light intensity of the intensity profile normal to the light sheet). This laser light sheet illuminates Duke Scientific 2-μm polystyrene spheres tracer particles in the liquid droplet. The liquid droplet is suspended by a small wire loop inside of a sealed $10\times10\times10$ cm^3 chamber. The transparent walls of the sample chamber allows the flow in the droplet to be visualized through a microscope with a long focal length lens and a CCD video camera. Reflected light from the particles and the droplet edge are focused into the camera. The images from the camera are recorded on a VCR and grabbed using an EPIX 4-Meg video board. Resultant images are analyzed with the help of image processing software. These images yield quantitative information about the velocity field, as shown in Fig. 2, through a technique known as particle displacement tracking. The volume and surface areas of the droplets are found from software where the user defines the symmetry axis of the droplet and then draws the edge of the droplet with a computer mouse. The volume and surface areas are then integrated and errors calculated.

transports momentum into the interior of the droplet and a convective (or Marangoni) flow results. Experimentally $\Delta\sigma$ is usually controlled through a temperature change that induces a temperature gradient perpendicular to the surface [$\Delta\sigma=(\Delta\sigma/\Delta T)\Delta T$, where $\Delta\sigma/\Delta T$ is a constant of the media that is usually negative). Although this ΔT results in a uniform surface temperature, ΔT still measures the magnitude of temperature change that a temperature perturbation would produce along the surface.

PROCEDURE AND APPARATUS

Our experiments are conducted at atmospheric pressure and room temperature in a sealed glass and metal chamber using methanol as our evaporating media as shown in Fig. 1. The chamber is in a temperature controlled room that allows a temperature variation of at most 0.1 °C inside the chamber over the ≈20 min needed to evaporate a droplet. This temperature variation is systematic over the ≈20-min cooling cycle of the room, indicating that the maximum temperature variation over ≈1 s is much lower. A methanol droplet is deployed, using a syringe, below a suspending loop approximately 1 mm in diameter. The surface tension at the loop, air, and methanol interface balances the weight of the droplet when the droplet is sufficiently small (≃2 mm in vertical length from the loop). The constraint of gravity forces us to use the suspending loop and the small scale droplet. This hanging droplet configuration also prevents an ideal spherical droplet from being realized: the hanging droplet is a more complicated oval-like shape that maintains roughly the same width as it evaporates while shrinking in vertical length. In addition to the shape distortion, the suspending loop introduces a thermal perturbation into the system. A better method for doing this experiment is to do it in a weightless or microgravity environment. To prevent surface contamination we first ultrasonically cleaned the chamber, syringe, suspending loop, etc., and then dried them in a vacuum oven. Light from a He-Ne laser is focused using a converging lens such that the waist of the beam occurs at the droplet. The beam then goes through a cylindrical lens to form a vertical light sheet as shown in Fig. 1. This light sheet is approximately 0.1 mm thick in the droplet. This laser light sheet illuminates Duke Scientific 2-μm polystyrene spheres tracer particles in the liquid droplet. The transparent walls of a sealed $10\times10\times10$ cm^3 sample chamber allows the flow in the hanging droplet to be visualized through a microscope with a long focal length lens and a charge coupled device (CCD) video camera. Reflected light from the particles and the droplet edge are focused into the camera. Resultant images are analyzed with the help of image processing software. We find that when a thermocouple is placed in the chamber with the laser sheet shining on it that the thermocouple increases in temperature by 0.9 °C in 2 min. Droplet convection visibly increases when the light sheet hits the suspending loop. In our experiments we block the light sheet so that it does not shine on the loop and we do not see any apparent difference in the convective behavior when the light sheet is on or off. Droplet velocity fields (see Fig. 2) and droplet edges (see Fig. 3) are then recorded as a function of time using a video frame grabber. The chamber is first flushed with air so that initially the methanol partial pressure in the external gas within the chamber is insignificant. The droplet is then deployed and the chamber sealed. As the droplet evaporates the relative humidity (RH) of methanol increases [relative humidity=(partial pressure of methanol)/(vapor pressure of methanol)]. By measuring the volume of the droplet, through image analysis of the axisymmetric droplet, we monitored the RH of the external gas in the chamber as the droplet evaporated. Typically the RH increases from 0% to 15% when one droplet evaporates in the sealed chamber. Figure 2 shows a typical velocity field inside of the droplet.

RESULTS AND DISCUSSION

Figures 2 and 3 show that significant and vigorous convection occurs inside of an evaporating droplet. The unsteady cellular structures, such as the ones shown in Fig. 3, tend to last ~1 s before they slow and stop. The cells always

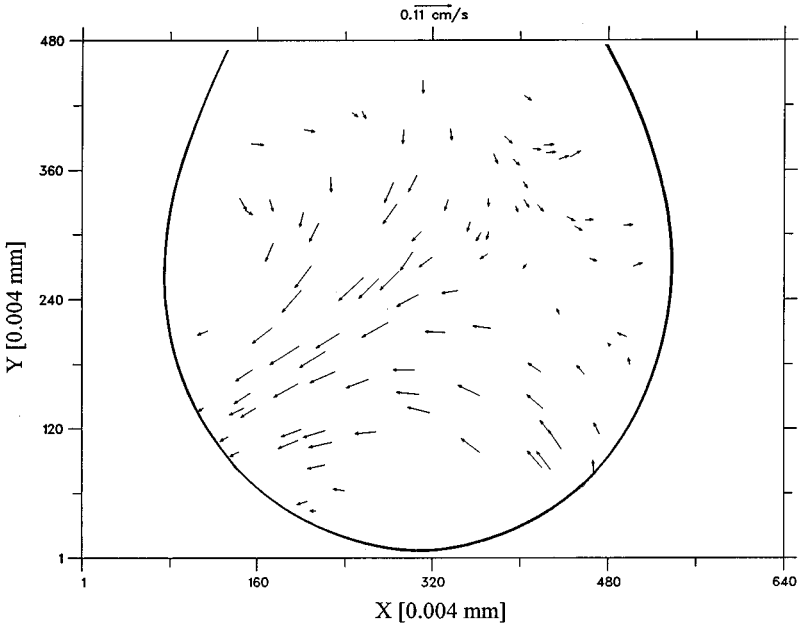

FIG. 2. The x and y components of the velocity field inside the center plane of an evaporating droplet. The droplet edge has been drawn to scale. Five consecutive images captured in a CCD camera were used to calculate the velocity field. Tracer particles (2 μm diameter) in a laser light sheet (100 μm thick) are imaged in the CCD camera. The axis of the camera lens is perpendicular to the light sheet. The suspending loop is above the droplet. These images yield quantitative information about the velocity field through a technique known as particle displacement tracking. Corrections have been made for light refraction at the axisymmetric droplet surface. The corrections for refraction change the magnitude and direction of the velocity vectors somewhat. The qualitative features of the flow cells are only slightly changed.

appear to form near the droplet surface, indicating that the driving force is produced at the surface by surface tension gradients. As shown in Figs. 2 and 3, the size of the cells generated by the localized surface tension gradients are of the order of the droplet radius. Cells appear to form at random at any place on the surface, although there is usually some delay before another cell forms in the same location. The cellular flow appears to be disordered in space and time. Figure 4 shows the surface area and volume as a function of time. In addition, the boundary condition at the surface

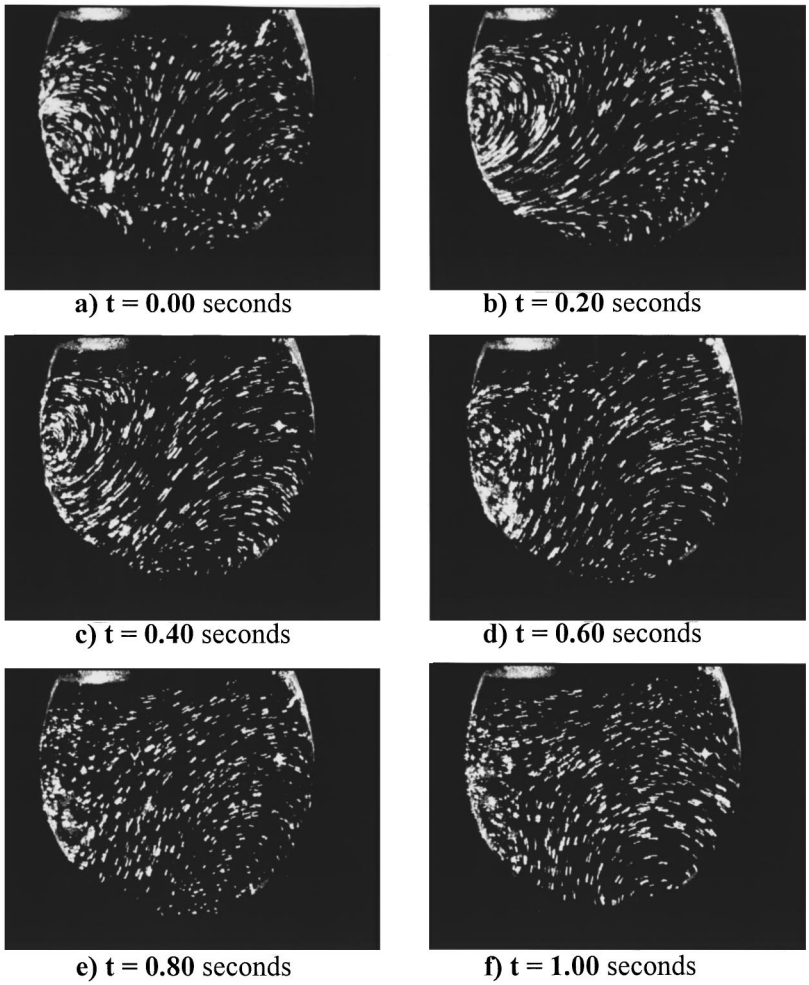

FIG. 3. Each of the six streak images of the droplet shown are made by exposing a moving tracer particle for 0.033 s and enhancing the resultant image. The suspending loop is above the droplet. The evolution of the flow is over 1 s with 0.20 s between images. This typical case starts with a cell that has just formed near the surface at the left. This cell exists for about 1 s before stopping while another cell forms elsewhere at the surface near the bottom right edge.

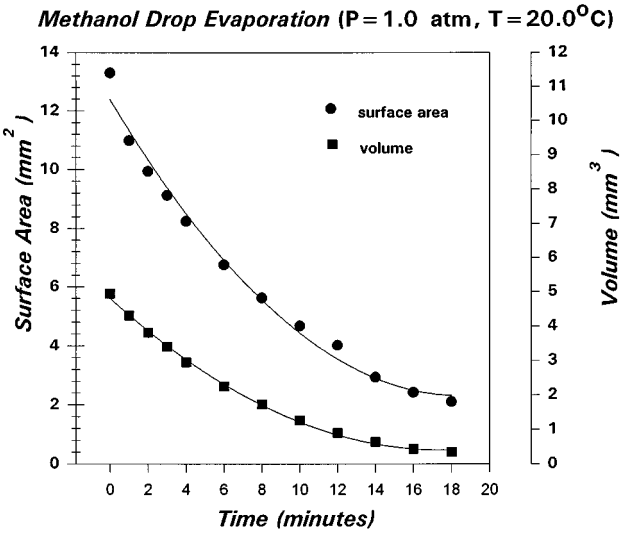

FIG. 4. By measuring the surface area and volume of a droplet at many different times using imaging software, the temporal evolution of these quantities is found. The surface area and volume tend to follow each other in time because of the geometrical constraint of the suspending loop, which maintains a roughly constant width while the droplet length decreases. The solid lines are shown as guides to the eye.

should lead to exterior convective transport. We did not have the ability to observe convective flow in the exterior of the droplet.

The evaporation rate decreases with increasing RH. The rate of cell formation and the particle speeds also decreased with increasing RH. In addition, we have observed, using the same experimental protocol, a slower evaporation rate in a water droplet that does not exhibit convection. We have also observed a higher evaporation rate in an acetone droplet that has stronger convection.

Although our data show that the interior convective heat transport to the droplet surface must play a large role in the evaporation process, to our knowledge, no one has ever considered it before. To include the convective effects we need to introduce a velocity scale. This is accomplished in the usual way by balancing the force per unit mass due to surface tension $\Delta\sigma/\rho R^2$, with the viscous force per unit mass $v(U/R^2)$ at the surface of the droplet to get the velocity scale $U=\Delta\sigma/\rho\nu$ [11]. This can also be rewritten in terms of Ma as $U=\mathrm{Ma}(\alpha/R)$. The heat out of the surface through evaporation is $(dm/dt)h_{lg}\sim\rho A(R/t)h_{lg}$ (where m is the mass of the droplet, t is the time, h_{lg} is the latent heat of vaporization per unit mass, and A is the area perpendicular to the heat flow). This output heat must be balanced by the heat into the surface. The heat into the surface includes both a heat conduction term $kA(dT/dr)\sim kA(\Delta T/R)$, where k is the thermal conductivity, and a heat convection term of order $\rho C_p U\Delta TA$, where C_p is the specific heat at constant pressure and U is the characteristic velocity. This balance implies that $R/t_c\sim(k/\rho C_p)(C_p\Delta T/h_{lg})(1/R)+U(C_p\Delta T/h_{lg})$, where t_c is the convective lifetime. $k/\rho C_p$ is just the thermal diffusivity α and the dimensionless combination $C_p\Delta T/h_{lg}$ is known as the Jacobs number J_a, which measures the ratio of heat conducted (per unit mass) $C_p\Delta T$ to the latent heat (per unit mass) h_{lg}. Using $R/t_c\sim\alpha J_a(1/R)+UJ_a$ and the above velocity scale we get $R/t_c\sim\alpha J_a(1/R)(1+M_a)$. This finally yields the convective lifetime $t_c\sim(R^2/\alpha J_a)[1/(1+M_a)]$. We note that the conductive lifetime t_l (at Ma=0 corresponding to no flow) is $t_l\sim R^2/\alpha J_a$.

TABLE I. Conductive lifetimes (t_l), convective lifetimes (t_c), and Marangoni numbers (Ma) at various temperature differences (ΔT). The convective lifetimes matches the data in Fig. 4 near the critical Marangoni number.

ΔT	t_l	t_c	Ma ($\mathrm{Ma}_c=80$)
4 °C	19.1 min	0.2 s	5585
1 °C	1.3 h	3.3 s	1396
0.5 °C	2.6 h	13.1 s	698
0.1 °C	12.8 h	5.4 min	140
0.06 °C	21.3 h	15.0 min	84
0.05 °C	25.5 h	21.6 min	70

Although our results show clearly that ΔT is an important parameter for the evaporation process, it has been previously ignored in this problem. Table I shows both the convective lifetime t_c and the conductive lifetime t_l of the methanol droplet for a range of ΔT values. The conductive lifetime t_l is in agreement with the data given in Fig. 4 ($\approx$18 min) for $\Delta T=4$ °C, which is equivalent to Ma=5585. This Ma is several orders of magnitude larger than the critical Marangoni number $\mathrm{Ma}_c=80$ [12]. Clearly a purely diffusive exterior mass transport and conductive interior heat transport should lead to a Marangoni flow. The large mass flux from convection inside of the droplet, as indicated in Figs. 2 and 3, makes it unlikely that such a large temperature change occurs. We have measured ΔT under different conditions using two small thermocouples, one inside the droplet and one just outside of the droplet. We have found that $\Delta T\approx 0.2$ °C just after the droplet is deployed using a different chamber that is operated below ambient pressure. At $\Delta T=0.06$ °C, $\mathrm{Ma}\simeq\mathrm{Ma}_c$ and t_c agrees with the data, which suggests that the droplet tends to a state of marginal stability. The interior heat transport from convection brings the droplet toward thermal equilibrium, while evaporation produces destabilizing temperature gradients at the surface. These two opposing tendencies keep the evaporating droplet system near a state of marginal stability. A small section of Marangoni unstable surface generates a cellular flow that transports the hot fluid to the cold side of the surface tension gradient. This convective heat transport decreases the surface tension gradient until the driving force and the cellular flow stops. This explains the cellular lifetime as the time required for hot fluid to move approximately one cycle in a convection cell and stabilize the surface tension gradient. The ~1-s convection cell lifetime is the time required for a hot fluid particle to travel ~1 mm at the speed of ~1 mm/s (see Fig. 2).

CONCLUSION

We have observed vigorous convection inside an evaporating droplet. This convection is disordered in space and

time and appears to be generated by local surface tension gradients. A simple scaling argument shows that the lifetime of the droplet is $(R^2/\alpha J_a)[1/(1+M_a)]$. This time scale agrees with our data when the system is near a state of marginal stability. This tendency to a state of marginal stability can be understood as the result of evaporation leading to Marangoni instability while the resulting strong convection leads to stability.

ACKNOWLEDGMENTS

We wish to thank J. C. Duh, V. Arpachi, and D. Beysens for stimulating discussions. This work was supported by NASA-JOVE.

[1] C. F. Bohren, *Clouds in a Glass of Beer* (Wiley, New York, 1987).
[2] R. Ristau, H. Iglseder, and H. L. Rath, ESA Report No. SP-295, p. 473, 1990 (unpublished).
[3] L. J. DeLucas and C. E. Bugg, J. Phys. D **26**, 100 (1993).
[4] K. A. White, NASA Report No. TM-89852, p. 1, 1987 (unpublished).
[5] J. C. Maxwell, Collect. Sci. Pap. Cambridge, **11**, 625 (1890).
[6] N. A. Fuchs, *Evaporation and Droplet Growth in Gaseous Media* (Pergamon, New York, 1959).
[7] G. Berg, M. Boudart, and M. Acrivos, J. Fluid Mech. **24**, 721 (1965).
[8] N. Zhang and W. Jang, J. Heat Trans. **104**, 656 (1982).
[9] J. R. Pearson, J. Fluid Mech. **4**, 489 (1958).
[10] A. Cloot and G. Lebon, Phys. Fluids A **2**, 525 (1990).
[11] V. J. Levich, *Physicochemical Hydrodynamics* (Prentice-Hall, Englewood Cliffs, NJ, 1962).
[12] M. F. Schatz, S. J. VanHook, J. B. Swift, W. D. McCormick, and H. L. Swinney, NASA Report No. CP-3276, p. 33, 1994 (unpublished).